THE JOURNAL OF PHYSICAL CHEMISTRY C

Article

pubs.acs.org/JPCC

Catalytic Activity of Au and Au_2 on the h-BN Surface: Adsorption and Activation of O_2

Min Gao,[†] Andrey Lyalin,*[,†,‡,§] and Tetsuya Taketsugu[†,‡]

[†]Division of Chemistry, Graduate School of Science, Hokkaido University, Sapporo 060-0810, Japan

[‡]Center for Strategic Utilization of Elements, Hokkaido University, Sapporo 060-0810, Japan

ABSTRACT: The structural, electronic, and catalytic properties of Au and Au_2 supported on the pristine and defected hexagonal boron nitride (h-BN) surface have been studied theoretically using density functional theory. It is demonstrated that adsorption and catalytic activation of O_2 on the h-BN supported Au and Au_2 can be affected by the interaction with the support via electron pushing and donor/acceptor mechanisms. It is shown that even weak interaction of Au and Au_2 with the defect-free "inert" h-BN surface can have an unusually strong influence on the binding and catalytic activation of the molecular oxygen. This effect occurs due to the mixing of the 5d orbitals of the supported Au and Au_2 with the N-p_z orbitals. Although the defect-free h-BN surface does not act as a good electron donor for the supported O_2–Au, it promotes an electron transfer from the Au to O_2, pushing electrons from the gold to the adsorbed oxygen. In the case of the defected h-BN surface, Au and Au_2 can be trapped effectively by N or B vacancy and impurity point defects. Strong adsorption on the surface defects is accompanied by the large charge transfer to/from the adsorbate. The excess of the positive or negative charge on the supported Au and Au_2 can considerably promote their catalytic activity. Therefore, the h-BN surface (pristine or defected) cannot be considered as an inert support for Au and Au_2.

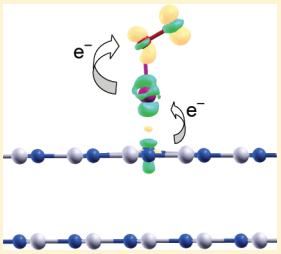

INTRODUCTION

Gold clusters supported on metal oxides possess unique catalytic activity in various oxidation reactions by molecular oxygen.[1−4] The high selectivity of gold clusters at mild temperatures makes them very attractive for many industrial applications.[5] It is commonly accepted that several factors can influence the catalytic activity of gold. One of the most important factors is the size effect. The catalytic activity of gold emerges when the size of clusters decreases down to 1−5 nm, while larger-sized particles and the bulk gold are catalytically inert.[1,2,6,7] Furthermore, supported gold clusters consisting of just a few atoms can also possess extraordinary high catalytic activity.[8] This is the regime where each atom counts and physical and chemical properties of clusters are extremely size sensitive and cannot be deduced from those known for larger sizes.[3,9,10]

Interaction with the support is another factor that can dramatically influence the chemical reactivity of gold clusters.[2,4,11−16] Most of the experimental studies have been performed for gold clusters supported on various metal oxides, such as MgO, ZnO, TiO_2, ZrO_2, Al_2O_3, and Fe_2O_3; see, e.g., ref 5 and references therein. It was demonstrated that the catalytic activity of gold clusters strongly depends on the type of the support material.[2,5,11] Interaction with the support can modify considerably the geometry structure and morphology of the supported cluster.[17,18] Charge transfer from the metal oxide support to the gold results in formation of the highly reactive charged gold clusters.[19,20] For example, in the case of catalytic oxidation by O_2, an electron from the negatively charged gold cluster readily transfers to the antibonding $2\pi^*$ orbital of the adsorbed O_2, which weakens the O−O bond and activates the oxygen molecule for further catalytic reaction or dissociation; see, e.g., refs 4, 21−25, and references therein. Such a mechanism of the charge-transfer-mediated activation and dissociation of O_2 on gold clusters has been intensively studied.[21,23−31] On the other hand, the positive charge accumulated on the gold can promote adsorption of some reactants, such as CO and hydrocarbons.[32,33] Thus, the charge state of the supported gold clusters can considerably influence their reactivity.[25,34] Catalytic activity of the supported clusters can also be promoted by defects in the support material. Defects can trap the metal cluster and enhance charge transfer between the support and the cluster. It was demonstrated that Au_8 clusters supported on the MgO(100) surface rich of F-center defects show high catalytic activity, while Au_8 deposited on the defect-poor MgO(100) surface is inert.[19,35] Defects are not the only factor responsible for charging of the supported metal clusters. Recently, it was demonstrated that the charge accumulated on the supported gold cluster can be tuned by varying the thickness of the metal oxide layer deposited on the metal support.[13,36−39] It is interesting that very small neutral gold clusters consisting of a few atoms are relatively inert as free species but can be catalytically active on the support. Thus, the support effects can play an even larger role in gold nanocatalysis than the particle size. On the other hand, it is commonly accepted that "inert" supports, such as hexagonal boron nitride (h-BN), do not affect the electronic and geometry structure of the supported clusters, and hence such clusters can be

Received: January 20, 2012
Revised: March 15, 2012
Published: April 5, 2012

   dx.doi.org/10.1021/jp300684v | *J. Phys. Chem. C* 2012, 116, 9054−9062

considered as pseudofree. This suggestion is widely used to study intrinsic properties of metal clusters that are free from the support effects.[7] Indeed, h-BN is an electrical insulator with a wide band gap (~5.8 eV) and high thermal and chemical stability.[40,41] It is unlikely that such a support can influence the physical and chemical properties of the deposited gold clusters.[42] However, very little attention has been paid to theoretical investigation concerning the role of the h-BN support on the catalytic properties of gold, with an exception of our recent work, where we have demonstrated that vacancy defects on the h-BN surface can functionalize small gold particles due to the electron transfer between the vacancy and the adsorbed gold.[43]

In the present paper, we report results of a systematic theoretical investigation of the structural, electronic, and catalytic properties of Au and Au_2 deposited on the pristine inert h-BN surface, as well as on the h-BN surface with B and N vacancy and impurity defects. We have selected the smallest gold particles Au and Au_2 as a simple model to elucidate the basic mechanisms of functionalization of gold on the inert h-BN support. The small free neutral gold clusters consisting of a few atoms are relatively inert toward O_2 activation and hence can serve as excellent model objects to study support effects. Adsorption and catalytic activation of O_2 on Au/h-BN and Au_2/h-BN are studied with the aim to understand the specific role played by the h-BN support in the catalytic processes on gold. It is demonstrated that two different mechanisms (electron pushing and donor/acceptor) can affect the catalytic properties of h-BN supported Au and Au_2. It is shown that the activity of Au and Au_2 toward O_2 catalytic activation can be sensitive to the interaction with the h-BN support even in the case of the ideal defect-free h-BN surface. Therefore, Au and Au_2 supported on the h-BN surface (pristine or defected) can not be considered as pseudofree particles. Such a phenomenon can be particularly important for understanding the mechanism of the catalytic activity of the supported small gold molecules in oxidation reactions employing molecular oxygen.

THEORETICAL METHODS

The calculations are carried out using density functional theory (DFT) with the gradient-corrected exchange-correlation functional of Wu and Cohen (WC)[44] as implemented in the SIESTA code.[45−47] The choice of WC functional is stipulated by the fact that it allows us to reproduce correctly the lattice constants, crystal structures, and surface energies of solids with layered structures like graphite or h-BN, whose distances between the layers are determined by rather weak interactions.[48] Thus, the standard Perdew−Burke−Ernzerhof (PBE)[49] functional which was successfully used to describe oxidation reactions on gold clusters supported on the MgO(001) surface[19] shows only marginal binding of the hexagonal layers in h-BN along c, while WC provides very accurate results that are close to experiment.[48] Moreover, the WC functional provides a realistic description of the binding energies and geometries of a h-BN layer on top of 3d, 4d, and 5d transition metal surfaces, correctly describing interaction of transition metals with h-BN.[48,50,51]

Double-ζ plus polarization function (DZP) basis sets are used to treat the $2s^22p^1$, $2s^22p^3$, $2s^22p^4$, and $6s^15d^{10}$ valence electrons of B, N, O, and Au atoms, respectively.[52,53] The remaining core electrons are represented by the Troullier−Martins norm-conserving pseudopotentials[54] in the Kleinman−Bylander factorized form.[55] All calculations are spin polarized. Relativistic effects are taken into account for Au via scalar-relativistic pseudopotentials. It has been shown that such an approach applied to gold describes correctly geometry and the electronic structure of small gold clusters and their alloys,[56,57] adsorption of Au to MgO surfaces,[58] as well as adsorption of O_2 and CO on small gold clusters.[23]

In the SIESTA code, the basis functions and the electron density are projected onto a uniform real-space grid. The mesh size of the grid is controlled by an energy cutoff, which defines the wavelength of the shortest plane wave that can be represented on the grid. In the present work, the energy cutoff of 200 Ry is chosen to guarantee convergence of the total energies and forces. A common energy shift of 10 meV is applied. The self-consistency of the density matrix is achieved with a tolerance of 10^{-4}. For geometry optimization, the conjugate-gradient approach was used with a threshold of 0.02 eV $Å^{-1}$. All energies are corrected for the basis set superposition errors (BSSEs). The atoms in molecules method of Bader (AIM) has been used for charge analysis.[59,60] The electron density has been plotted using the XCRYSDEN visualization program.[61]

Periodic boundary conditions are used for all systems, including free molecules and clusters. In the latter case, the size of a supercell was chosen to be large enough to make intermolecular interactions negligible. To validate our approach and choice of WC functional, we have calculated the dissociation energies and interatomic distances for O_2 and Au_2 diatomic molecules. Our calculations demonstrate that the dissociation energy, D_e, and bond length in O_2 (5.88 eV, 1.24 Å) and Au_2 (2.28 eV, 2.55 Å) are in good agreement with experimental data for O_2 (5.23 eV, 1.21 Å) and Au_2 (2.29 eV, 2.47 Å).[62] The h-BN lattice has been optimized using the Monkhorst−Pack[63] 10 × 10 × 4 k-point mesh for Brillouin zone sampling. The calculated lattice parameters $a = b = 2.504$ Å and $c = 6.656$ Å are in excellent agreement with the experimental values of $a = b = 2.524 \pm 0.020$ Å and $c = 6.684 \pm 0.020$ Å, reported in ref 64. The h-BN surface is represented by the two-layer slab containing 7 × 7 unit cells (98 units of BN per slab) with the surface area of 3.07 nm^2. The periodically replicated slabs are separated by the vacuum region of 25 Å in the (001) direction. In all calculations, the bottom layer in the slab is fixed, and all other atoms are fully relaxed. Only the Γ point is used for sampling the Brillouin zone due to the large size of the supercell.

THEORETICAL RESULTS

Surface Model and Adsorption of Au and Au_2 on the Defect-Free and Defected h-BN. The h-BN lattice has a layered structure which is very similar to graphite. The planar networks of B_3N_3 hexagons are regularly stacks on top of each other.[65] Due to the partially ionic character of the B−N bonding, the B atoms in one layer are located on top of the N atoms of the neighboring layer and vice versa, as shown in Figure 1(a).

In the present work, we study adsorption of Au and Au_2 on the defect-free h-BN surface as well as h-BN surfaces with boron vacancy (V_B), nitrogen vacancy (V_N), nitrogen impurity (N_B), and boron impurity (B_N) point defects, which are schematically shown in Figure 1(b). These are the simplest and relatively stable types of defects in h-BN. It is important to note that spontaneous magnetization of the lattice can occur in systems with point defects such as impurities or vacancies.[66] Thus, we have found that the considered systems with V_B and

dx.doi.org/10.1021/jp300684v | J. Phys. Chem. C 2012, 116, 9054−9062

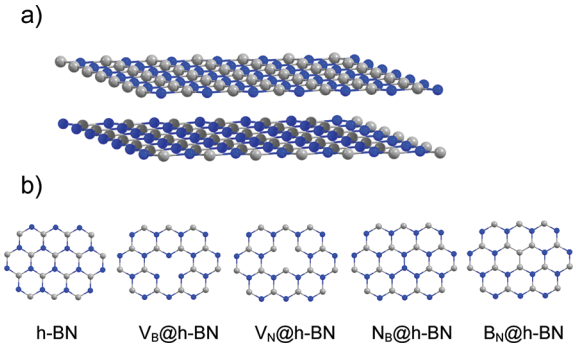

Figure 1. h-BN surface models: (a) side view of the two-layer h-BN p(7 × 7) slab; (b) schematic presentation of the defect-free h-BN surface and h-BN surface with boron vacancy (V_B), nitrogen vacancy (V_N), nitrogen impurity (N_B), and boron impurity (B_N) defects (only part of the top layer is shown).

V_N vacancy defects are in the quartet and doublet spin states, respectively. The enhancement of the spin polarization on V_B and V_N defects in the h-BN monolayer has recently been reported in ref 66.

The stability of point defects in the h-BN surface has been intensively investigated. It was demonstrated that N_B and B_N impurity defects have low formation energies, comparable to those of the vacancies V_N and V_B.[67,68] Thus, it was found that N_B is the most stable defect in h-BN under N-rich conditions followed by the nitrogen vacancy.[67] This is consistent with experimental findings of large concentrations of nitrogen interstitials and vacancies and of the trapping of nitrogen in the hexagonal phase of BN thin films grown by ion-bombardment-assisted deposition techniques; see ref 67 and references therein. The stability of divacancies in graphitic boron nitride (g-BN) sheets has been studied in ref 69. It was shown that the divacancies are more frequently formed in graphene than in the g-BN.[69] However, it was found that in the BN single-wall nanotubes the most stable type of point defect is the BN divacancy.[70] Formation of the triangle defects in the h-BN monolayer has also been investigated; see, e.g., refs 71, 72, and references therein. It was demonstrated that N(B) triangle defect states of the h-BN atomic layer with N(B) edge atoms have acceptor (donor) levels.[72] Cohesive energy calculations indicate that the h-BN atomic layer with N triangle defects is more or less stable, respectively, than that with B triangle defects when it is negatively or positively charged.[72] The relative stability of the particular type of defects in h-BN often depends on the experimental conditions and the environment. Therefore, in the present work, we study only the simplest types of point defects in h-BN.

To obtain the most stable geometries of Au and Au_2 supported on the h-BN surface, we have created a large number of starting configurations by adding gold particles with different orientation with respect to the surface. These structures have been fully optimized on the surface, with accounting for relaxation of all gold atoms as well as the top layer of h-BN. The bottom layer of h-BN in the slab was fixed. Thus, we have taken into account structural relaxations on the h-BN surface due to its interaction with the supported gold particles. A similar approach has been used in our recent work to describe interaction of Au, Au_2, Au_8, and Au_{20} with the TiO_2 rutile support.[43,73] Figure 2 presents the optimized geometries of Au and Au_2 adsorbed on the defect-free and defected h-BN surface. In the case of the defect-free h-BN surface, both Au and Au_2 adsorb on top of the N atom. Figure 2 demonstrates that Au adsorbs on top of V_B, V_N, and N_B point defects and bridges boron impurity with the nearest boron atom in the case of the B_N defect. Gold dimer adsorbs either vertically (defect-free h-BN and N_B@h-BN) relative to the surface plane or inclined from the surface normal (V_B@h-BN, V_N@h-BN, and B_N@h-BN). Note that the defected h-BN surface undergoes structural relaxations upon Au and Au_2 adsorption which are especially strong for B_N@h-BN. The total spin state of the considered systems is a singlet for Au/V_N@h-BN, Au_2/h-BN, Au_2/N_B@h-BN, and Au_2/B_N@h-BN; a doublet for Au/h-BN, Au/N_B@h-BN, Au/B_N@h-BN, Au_2/V_B@h-BN, and Au_2/V_N@h-BN; and a triplet for Au_2/V_B@h-BN.

Figure 3 presents the calculated binding energy of Au and Au_2 to the defect-free and defected h-BN surface. The binding energy of a gold cluster Au_n consisting of n atoms to the pristine and defected h-BN surface is defined as

$$E_b(\mathrm{Au}_n/\text{h-BN}) = E_{tot}(\mathrm{Au}_n) + E_{tot}(\text{h-BN}) - E_{tot}(\mathrm{Au}_n/\text{h-BN}) \quad (1)$$

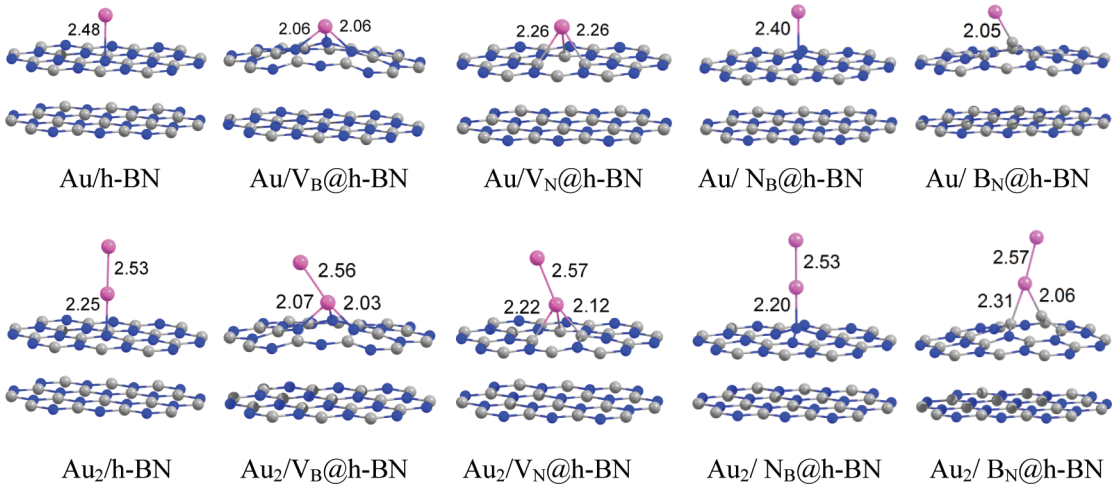

Figure 2. Optimized geometries of Au and Au_2 adsorbed on the defect-free h-BN surface, as well as on the h-BN surface with V_B, V_N, N_B, and B_N point defects. The interatomic distances are given in Angstroms. Only part of the h-BN slab is shown.

dx.doi.org/10.1021/jp300684v | J. Phys. Chem. C 2012, 116, 9054−9062

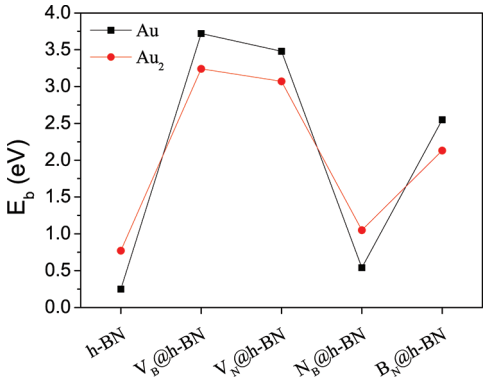

Figure 3. Calculated binding energy of Au and Au_2 to the pristine and defected h-BN surfaces.

where $E_{tot}(Au_n/h\text{-}BN)$ denotes the total energy of the Au_n/h-BN system, while $E_{tot}(Au_n)$ and $E_{tot}(h\text{-}BN)$ are the total energies of the noninteracting Au_n cluster and h-BN slab, respectively.

Our calculations confirm that Au and Au_2 interact weakly with the pristine h-BN surface. Thus, the calculated binding energies of Au and Au_2 on h-BN are $E_b(Au/h\text{-}BN) = 0.25$ eV and $E_b(Au_2/h\text{-}BN) = 0.77$ eV, respectively. However, the interaction of Au and Au_2 with the support becomes considerably stronger when the h-BN surface contains V_B, V_N, and B_N point defects. Thus, nitrogen and boron vacancy defects trap the gold atom with the binding energy of 3.48 and 3.72 eV, respectively. The gold dimer adsorbs on V_N and V_B with the binding energy of 3.07 and 3.24 eV, respectively.

We found that there is little charge transfer from the pristine h-BN surface to the adsorbed gold. According to the Bader analysis, the charges localized on the adsorbed Au and Au_2 are −0.08e and −0.14e, respectively, where e is an elementary charge.

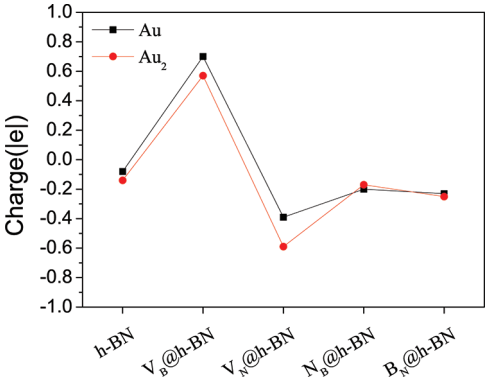

Figure 4. Calculated Bader charge localized on Au and Au_2 adsorbed on the pristine and defected h-BN surfaces.

The vacancy and impurity defects in the h-BN surface influence considerably its electronic structure. Thus, the considerable reduction in the work function of defected h-BN monolayers was demonstrated with an exemption of V_B.[66] Figure 4 demonstrates that the strong adsorption on vacancy defects is accompanied by the large charge transfer to/from the gold particles. Thus, the Bader charges localized on Au trapped by V_N and V_B defects are −0.39e and +0.70e, respectively. The gold dimer adsorbed on V_N and V_B defects possesses Bader charge of −0.59e and +0.57e, respectively. It is important to note that the charge of the adsorbed gold particles strongly depends on the type of vacancy defects and can possess either negative or positive values. Thus, V_N, N_B, and B_N donate electrons to the adsorbed Au and Au_2, while V_B acts as an electron acceptor. Hence, it is possible to modify considerably the cluster's electron donor−acceptor capacity and its catalytic properties by the support design.

Adsorption and Activation of O_2 on Au/h-BN and Au_2/h-BN. One can suggest that catalytic activity of Au and Au_2 supported on the defect-free h-BN surface is not affected by the interaction with the support, while adsorption of gold particles on the defected h-BN surface might result in a strong change in their catalytic activity. However, our calculations show that in the case of the defect-free h-BN support the ability of small gold particles to activate the molecular oxygen can be changed dramatically. To demonstrate this unexpected effect and to study the specific role played by the h-BN support in formation of catalytic properties of the small gold particles, we perform systematic investigation of adsorption and activation of O_2 on Au/h-BN and Au_2/h-BN systems.

Adsorption of molecular oxygen on free gold clusters has been intensively investigated; see, e.g., refs 3, 4, 21−24, 29, and references therein. It was found that O_2 readily adsorbs and becomes catalytically activated on small neutral gold clusters with an odd number of atoms as well as on gold cluster anions; see, e.g., ref 3 and references therein. Such an ability of small gold clusters to bind and activate molecular oxygen has been explained by the transfer of unpaired valence electron from the cluster to the oxygen antibonding $2\pi^*$ orbital, see, e.g., refs 3, 4, 21−24, and references therein. Our calculations demonstrate that O_2 adsorbs on the free Au and Au_2 with the binding energy of 0.49 and 0.48 eV, respectively. The O−O bond length enlarges from 1.24 Å (free O_2) to 1.27 Å and 1.26 Å, upon O_2 adsorption on the gold monomer and dimer, respectively. A slight increase in the O−O bond length of the adsorbed O_2 demonstrates its catalytic activation. It is important to note that the correct description of interaction between O_2 and a single Au atom is a rather difficult problem for DFT.[31] The popular PBE, PW91, and TPSS functionals do not show good performance and overestimate binding of O_2 to Au. It was demonstrated that to obtain accurate results for O_2−Au interaction the functionals used have to be able to treat the long-range interaction well.[31] Although the WC functional used in the present work overestimates binding of O_2 to Au, it is a good compromise choice for simultaneous discription of the O_2−Au and Au−h-BN interactions, as well as a weak long-range interaction between layers in h-BN. Moreover, in the present work we are interested not in the exact values of O_2 adsorption energy but in a relative change of adsorption energies due to the support effect. For this task, the choice of the DFT functional is not so critical, and the WC functional gives a qualitatively correct description of the process.

Can h-BN support modify the catalytic properties of gold? Our calculations demonstrate that O_2 readily adsorbs on Au and Au_2 supported on the pristine and defected h-BN surface. Figure 5 presents optimized geometries of O_2 adsorbed on $Au_{1,2}$/h-BN, $Au_{1,2}/V_B$@h-BN, $Au_{1,2}/V_N$@h-BN, $Au_{1,2}/N_B$@h-BN, and $Au_{1,2}/B_N$@h-BN systems. It is seen from Figure 5 that the oxygen molecule adsorbs on top of the Au atom supported on the defect-free h-BN surface and trapped by the V_B, N_B, and B_N defects but bridges Au and the surface B atom in the case of O_2 adsorption on the Au/V_N@h-BN center. O_2 adsorbs on Au_2/h-BN, similar to the case of the free Au_2, forming the angle

dx.doi.org/10.1021/jp300684v | J. Phys. Chem. C 2012, 116, 9054−9062

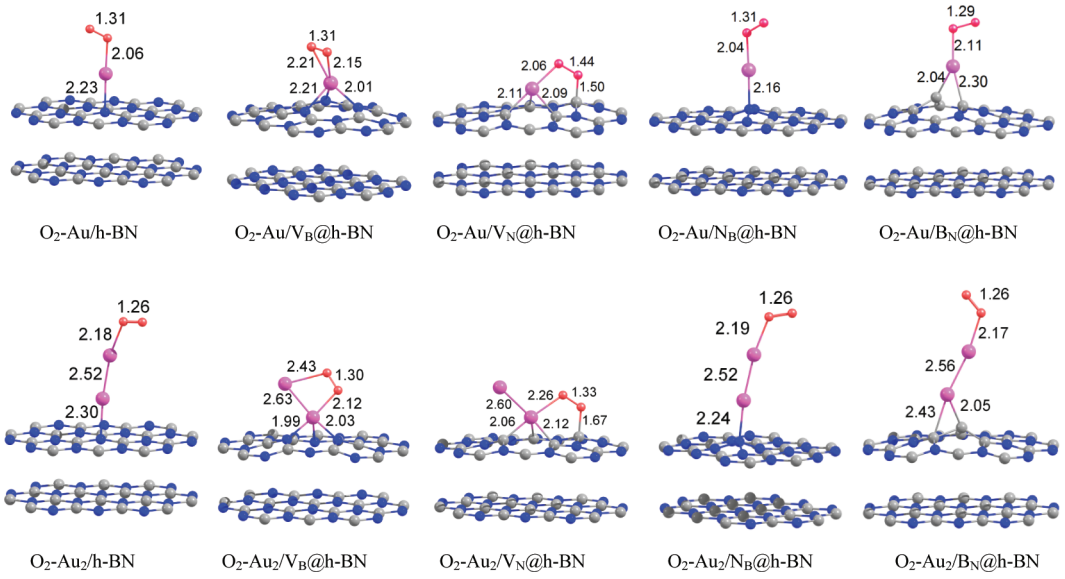

Figure 5. Optimized geometries of O_2 adsorbed on the supported Au and Au_2. The interatomic distances are given in Angstroms. Only part of the h-BN slab is shown.

of 106° between the O−O and Au−Au bonds. However, in the case of the Au_2/V_B@h-BN system, O_2 bridges two gold atoms, while for the Au_2/V_N@h-BN system, O_2 bridges nearest to the surface Au atom, which is located on top of V_N and B atom on the surface. Therefore, an interface between the supported gold cluster and the h-BN surface might play an important role in oxidation reactions on h-BN supported gold clusters. This suggestion requires further theoretical and experimental investigation that goes far beyond the aims of the present study.

It is seen from Figure 5 that the interaction of Au and Au_2 with the support results in additional activation of the adsorbed O_2 and weakening of the O−O bond. This effect is especially strong for V_N vacancy defect, which acts as an electron donor for the supported Au and Au_2. Figure 5 demonstrates that the O−O bond length in adsorbed O_2 is enlarged similar to the superoxide state (the calculated O−O bond length in O_2^- is 1.38 Å), with an exception of O_2−Au_2/h-BN, O_2−Au_2/N_B@h-BN, and O_2−Au_2/B_N@h-BN, where interaction of Au_2 with the support does not lead to additional activation of O_2. We found that O_2 adsorbs on the supported Au atoms (all considered supports) and Au_2 dimers trapped by the V_B and V_N defects in the singlet spin state, while O_2 adsorbed on Au_2/h-BN, Au_2/N_B@h-BN, and Au_2/B_N@h-BN is in the triplet state.

The results of our calculations demonstrate that interaction of Au with the inert defect-free h-BN surface can lead to a dramatic change in the ability of gold to activate the adsorbed O_2. In addition, the presence of the vacancy and impurity point defects on the h-BN surface results in a drastic change in the charge state of the trapped Au and Au_2 and hence also influences the catalytic activity of the supported gold particles. Although it is well established that F-center defects in metal-oxides can promote catalytic activity of gold clusters via the charge transfer,[19,35,74] to the best of our knowledge the similar effect for gold clusters supported on the h-BN surface has not been studied yet.

Figure 6 presents the calculated binding energy of O_2, to the free and h-BN supported Au and Au_2. We found that O_2 adsorbs on the free Au and Au_2 with the binding energy of 0.49 and 0.48 eV, respectively. It is seen from Figure 6 that interaction of Au and Au_2 with the h-BN support results in the

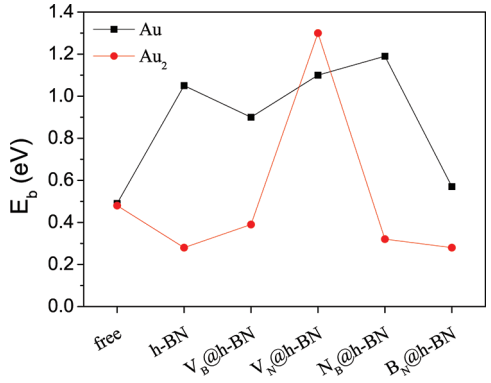

Figure 6. Binding energy of O_2 to the free and supported Au (filled squares) and Au_2 (filled dots).

considerable change in oxygen binding. Thus, O_2 adsorbs on Au/h-BN, Au/V_B@h-BN, Au/V_N@h-BN, and Au/N_B@h-BN with binding energies of 1.05, 0.90, 1.10, and 1.19 eV, respectively. This is two times larger than the binding energy of O_2 to the free Au. Although the strong binding of O_2 to Au trapped by V_B, V_N, and N_B defects can be explained by the large charge transfer between the corresponding vacancy defects and the trapped Au atom, the giant increase in binding energy of O_2 to a gold atom supported on the defect-free h-BN surface is surprising. Indeed, the gold atom interacts weakly with the defect-free h-BN surface, and hence, one can expect that the role of the h-BN support in oxygen binding to Au/h-BN is negligible. Our calculations clearly demonstrate that this suggestion is not correct. It is interesting that binding of O_2 to Au_2/h-BN and Au_2 trapped by V_B, N_B, and B_N defects is weaker if compared with free Au_2Au_2. However, adsorption of O_2 on the Au_2/V_N@h-BN center is highly promoted. In the latter case, O_2 bridges one of the gold atoms and the nearest boron atom on the surface, with binding energy of 1.30 eV. Thus, the oxygen binding to the supported gold particles considerably depends on the number of gold atoms and the type of support.[75]

dx.doi.org/10.1021/jp300684v | J. Phys. Chem. C 2012, 116, 9054−9062

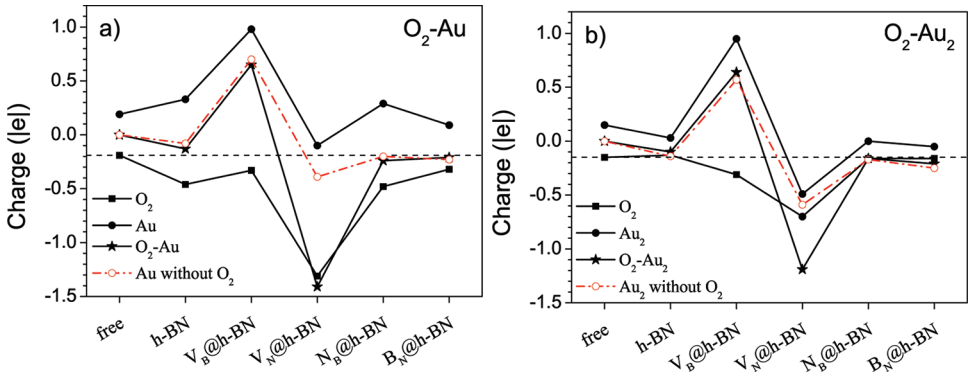

Figure 7. (a) Charge localized on O_2 (filled squares), Au (filled dots), and the total charge on O_2−Au (filled stars) for the free and supported O_2−Au system; charge localized on Au without adsorbed O_2 (open dots). (b) Charge localized on O_2 (filled squares), Au_2 (filled dots), and the total charge on O_2−Au_2 (filled stars) for free and supported O_2−Au_2 system; charge localized on Au_2 without adsorbed O_2 (open dots). Horizontal dashed lines indicate charge on the oxygen molecule adsorbed on a free Au (a) and Au_2 (b).

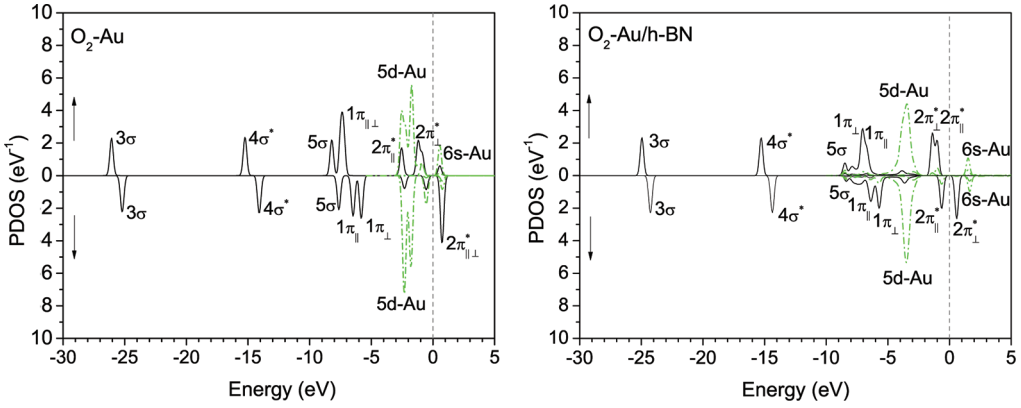

Figure 8. Partial density of electronic states (PDOS) projected on the O_2 molecule (solid line) and Au atom (dashed line): O_2 adsorbed on Au atom (left) and O_2 adsorbed on h-BN supported Au atom (right). The location of the Fermi level is indicated by a dashed vertical line at 0 eV. A Gaussian broadening of half-width 0.2 eV has been used.

Activation and reactivity of the adsorbed O_2 are strongly affected by the charge transfer from the gold hybridized 5d6s orbitals to the antibonding $2\pi^*$ orbital of O_2. Figure 7 demonstrates how the Bader charges localized on O_2, Au, and Au_2 in O_2−Au and O_2−Au_2 systems depend on the support. In Figure 7, lines with filled squares represent the Bader charge localized on O_2 in free and supported O_2−$Au_{1,2}$ systems, while lines with filled dots represent the Bader charge on Au and Au_2. Lines with filled stars represent the total charge of O_2−Au and O_2−Au_2 systems that corresponds to the total electron transfer from the support to the adsorbate. Lines with open dots represent the charge localized on the supported Au and Au_2 without coadsorbed O_2.

In the case of O_2 adsorption on free Au, the Bader charge localized on O_2 is −0.19e. Figure 7(a) demonstrates that interaction of Au with the defect-free h-BN support results in the drastic increase in charge transfer to the adsorbed O_2. Thus, the charge localized on O_2 in the O_2−Au/h-BN system is −0.46e, which is more than twice as large if compared with the case of unsupported O_2−Au. As discussed above, the adsorption of Au on the defect-free h-BN is accompanied by the small electron transfer from the surface to the gold atom, equal to −0.08e. Adsorption of O_2 on Au/h-BN results in a slight increase of the charge transfer from the support to O_2−Au, which is equal to −0.13e. However, the drastic increase in the charge localized on O_2 in O_2−Au/h-BN cannot be explained only by the charge transfer from the support. That means that the interaction of Au with the defect-free h-BN support considerably promotes the charge transfer from Au to O_2. Such an effect becomes even more clear for O_2 adsorbed on the Au/V_B@h-BN center. As we have discussed above, the B vacancy acts as an electron acceptor. Thus, Au trapped by the V_B@h-BN defect possesses a positive charge. It is well-known that free gold cluster cations are inert toward molecular oxygen. However, our calculations demonstrate that O_2 readily adsorbs and becomes highly activated on the positively charged Au/V_B@h-BN center. Figure 7(a) demonstrates that interaction with the V_B@h-BN support promotes additional charge transfer (in comparison with O_2 adsorbed on free Au) from the gold to the adsorbed O_2, even if the adsorbed Au has a positive charge. This effect is rather similar to that of promotion of oxygen activation by the small gold clusters with coadsorbed hydrogen[76] or ethylene[25] molecules. In the case of O_2 adsorption on the Au/V_N@h-BN center, a gold atom trapped by the N vacancy has a negative charge. That promotes charge transfer to the adsorbed O_2. However, in contrast to the Au/h-BN, Au/V_B@h-BN, Au/N_B@h-BN, and Au/B_N@h-BN centers, in the case of O_2 adsorption on the Au/V_N@h-BN center, the additional charge transfer to the oxygen occurs mainly due to the charge transfer from the support.

It is seen from Figure 7(b) that the interaction of Au_2 with the defect-free h-BN does not lead to any additional charge transfer to the adsorbed O_2. However, adsorption of O_2 on Au_2/V_B@h-BN is accompanied by the additional charge

dx.doi.org/10.1021/jp300684v | J. Phys. Chem. C 2012, 116, 9054−9062

transfer from Au_2, while the total charge transfer from the V_B@h-BN support to the Au_2 and O_2−Au_2 adsorbates remains unchanged. Hence, interaction of Au_2 with the V_B defect promotes charge transfer from the gold to the oxygen. However, in the case of O_2 adsorption on the Au_2/V_N@h-BN center, an additional charge transfer to O_2 occurs mainly due to the charge transfer from the V_N@h-BN surface, but not from the gold dimer. In both cases, charge transfer to O_2 is accompanied by its strong activation.

Thus, we demonstrated that interaction of Au and Au_2 with the pristine and defected h-BN surface strongly influence adsorption and catalytic activation of O_2. Although one can expect that the defected h-BN surface can influence the ability of the supported gold to activate the adsorbed O_2, a similar effect found for the pristine h-BN surface is surprising. To gain more insight into the origin of the unusual activity of Au supported on the defect-free h-BN surface, we present the partial density of electronic states (PDOS) projected on the O_2 molecule and Au atom for O_2−Au (Figure 8, left) and O_2−Au/h-BN (Figure 8, right) systems. The maxima of the PDOS corresponding to the O_2 molecule adsorbed on the free and h-BN supported Au atom can be assigned to the peaks of the PDOS spectra of the free O_2 (see Figure 8). Bonding of O_2 to the gold atom involves mixing of the 1π and $2\pi^*$ orbitals of the adsorbed O_2 with the 5d and 6s orbitals of gold. One can notice a prominent splitting of the 1π and $2\pi^*$ orbitals on the "parallel", $\pi_{\parallel}$, and "perpendicular", $\pi_{\perp}$, components, where the corresponding orbitals of π character close to the O_2 molecule lie in the plane ($\pi_{\parallel}$) and perpendicular ($\pi_{\perp}$) to the plane defined by the O_2 and Au.[21]

The down-spin $2\pi^*$ orbital of free O_2 is unoccupied and located above the Fermi level. Adsorption of O_2 on the free Au atom leads to the appearance of the partly filled down-spin s +$2\pi^*$ and d+$2\pi^*$ components in the PDOS spectra and depopulation of the 6s orbital of gold. Partial population of the antibonding $2\pi^*$ orbital of O_2 is responsible for the catalytic activation of the adsorbed oxygen and stretching of the O−O bond. Such a mechanism of activation of the oxygen molecule adsorbed on small gold clusters has been extensively described in the literature.[3,21]

Bonding of Au to the defect-free h-BN surface is mainly driven by mixing of N-p_z with metal-d_{z^2} orbitals. Interaction of Au with the defect-free h-BN surface results in a broadening of the d_{z^2} PDOS and its overlapping with the N-p_z PDOS. A similar effect of mixing of N-p_z and B-p_z orbitals of the h-BN monolayer with d_{z^2} orbitals of 3d, 4d, and 5d transition metals is responsible for binding of the h-BN monolayer to metal surfaces.[50]

Figure 8 demonstrates a wide broadening of the 5d peak of the supported Au resulting in overlapping of the 5d states of Au with the 5σ and 1π states of the adsorbed O_2. This effect leads to a strong mixing of the 5d states of Au with the 5σ and 1π states of O_2. Thus, interaction of Au with the h-BN support promotes mixing of Au and O_2 states. Moreover, such an interaction leads to the population of the down-spin $2\pi^*$ orbital of O_2 and complete depopulation of the 6s orbital of Au. Population of the $2\pi^*$ state results in the additional activation of O_2 adsorbed on the Au/h-BN center in comparison with the free Au atom. Thus, interaction of Au with the defect-free h-BN surface leads to the strong promotion of binding and catalytic activation of the adsorbed O_2. This is a rather surprising effect because it is widely believed that h-BN support is inert. Indeed, Au adsorbs weakly on the h-BN surface with the binding energy of 0.25 eV, and O_2 does not bind to h-BN at all. Nevertheless, mixing of the 5d states of the supported Au with N-p_z states of h-BN results in a strong modification of the Au-5d states, which in turn influence the adsorption of O_2 on the supported Au.

Figure 9 demonstrates isosurfaces of the electron density difference in O_2−Au induced by the interaction of Au with the h-BN surface. We find that the distribution of the electron density in the free and h-BN supported O_2−Au systems differs considerably. As we have discussed above, the interaction of the Au atom with the h-BN support results in an additional charge transfer to the adsorbed O_2 in the O_2−Au/h-BN system. Interestingly, that additional charge transfer to the oxygen molecule adsorbed on Au/h-BN occurs mainly from the Au atom itself, but not from the h-BN surface. Thus, the defect-free h-BN surface does not work as a good electron donor (the h-BN surface donates only −0.1e to the supported O_2−Au), but it promotes an electron transfer from Au to O_2, pushing electrons from gold to oxygen. Figure 9 shows that the isosurface of an excess of the electron density localized on O_2 is similar to the electron distribution of the $2\pi_{\parallel}^*$ orbital in O_2, while the plot of the electron density loss on the Au atom is similar to the hybridized 5d6s-Au orbital. Note that there is also small electron density loss localized on the N atom directly interacting with Au. This electron loss corresponds to the small electron transfer from h-BN to the supported O_2−Au.

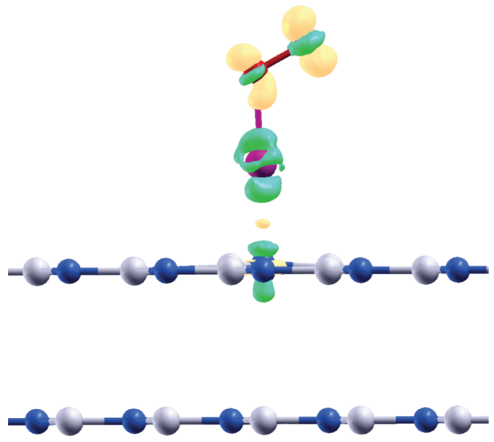

Figure 9. Isosurfaces of the electron density difference in O_2−Au induced by the interaction of Au with the h-BN surface, i.e., $\rho_{tot}(O_2\text{−Au/h-BN}) - \rho_{tot}(O_2\text{−Au}) - \rho_{tot}(\text{h-BN})$. Yellow regions correspond to excess electronic charge, and green ones correspond to electron loss. The contours shown are at +0.006 and −0.006 electrons per Å^3.

CONCLUSIONS

In summary, the present theoretical study demonstrates that the ability of Au and Au_2 to activate the adsorbed O_2 is sensitive to the interaction with both defect-free and defected h-BN support. There are two different mechanisms responsible for such a support effect. The first one we call an electron pushing mechanism, and the second one is a donor/acceptor mechanism.

It is commonly believed that the pristine defect-free h-BN surface is an inert support for metal particles. Indeed, we have found that Au and Au_2 interact weakly with the regular defect-free h-BN surface. However, this weak interaction of gold particles with h-BN support leads to the strong promotion of binding and catalytic activation of O_2 adsorbed on Au/h-BN.

dx.doi.org/10.1021/jp300684v | J. Phys. Chem. C 2012, 116, 9054−9062

On the other hand, adsorption of O_2 on Au_2/h-BN is suppressed, if compared with the case of free Au_2. It is demonstrated that this interesting novel and unexpected effect occurs due to the mixing of the 5d states of the supported Au and Au_2 with N-p_z states. Such a mixing is responsible for bonding of Au and Au_2 to the surface of h-BN and results in a strong modification of the Au-5d orbitals. Rearrangement of the Au-5d orbitals strongly influences the adsorption and activation of O_2 on the h-BN supported gold particles. It is shown that although the defect-free h-BN surface does not act as a good electron donor for the supported O_2−Au it promotes an electron transfer from the supported Au to O_2, pushing electrons from the gold to the oxygen.

In the case of the defected h-BN surface, the supported Au and Au_2 can be trapped effectively by N or B vacancy defects. Strong adsorption on the surface defects is accompanied by the charge transfer to/from the adsorbate. The value and the sign of the charge accumulated on the adsorbate depend on the adsorption sites. Thus, V_N, N_B, and B_N donate electrons to the adsorbed Au and Au_2, while V_B acts as an electron acceptor. The excess of the positive or negative charge on the supported gold clusters can considerably promote their catalytic properties and enhance activation of the adsorbed O_2.

Our finding leads to a very important conclusion that Au and Au_2 supported on the h-BN surface (pristine or defected) can not be considered as pseudofree particles. The support effects have to be taken into account, even when the interaction of the pure gold particles with the support is weak. Thus, even inert support can count.

In the present paper, we have elucidated mechanisms of adsorption and catalytic activation of O_2 on the smallest gold particles—Au and Au_2. Activation of the molecular oxygen is the first step in further oxidation reactions that can occur via either O_2 dissociation and further oxidation of the reactant by the atomic oxygen or direct oxidation of the reactant by the activated molecular oxygen. The effect of the h-BN support on dissociation of the adsorbed O_2 and direct oxidation of simple model molecules such as CO by activated molecular O_2 will be investigated in a further study. Another important problem is to investigate how the h-BN support influences the catalytic properties of gold clusters of larger sizes up to 1−5 nm, where the strong size-dependence of the catalytic activity of gold clusters has been observed experimentally. One can suggest that mixing of the N-p_z and B-p_z orbitals of h-BN with d_{z^2} orbitals of gold can modify the local electronic structure of the gold atoms in the contact area between the cluster and the support. As it is known, such an interface can play a crucial role in catalytic activity of the supported clusters.[15,73,77] Therefore, it is nessesary to clarify whether or not the perimeter interface between the cluster and the h-BN support affects the catalytic activity of gold clusters. Understanding the mechanisms that influence the catalytic activity of supported clusters is a priority task.

AUTHOR INFORMATION

Corresponding Author

*E-mail: lyalin@mail.sci.hokudai.ac.jp.

Notes

The authors declare no competing financial interest.

[§]On leave from: V. A. Fock Institute of Physics, St. Petersburg State University, 198504 St. Petersburg, Petrodvorez, Russia.

ACKNOWLEDGMENTS

This work was supported by the Global COE Program (Project No. B01: Catalysis as the Basis for Innovation in Materials Science) from the Ministry of Education, Culture, Sports, Science and Technology, Japan; the Grant-in-Aid for the Project on Strategic Utilization of Elements; the JSPS Grant-in-Aid for Scientific Research C; and the Collaborative Research Program 2011, Information Initiative Center, Hokkaido University, Sapporo, Japan. The computations were partly performed using the Research Center for Computational Science, Okazaki, Japan. We wish to thank Professor K. Uosaki (NIMS, Tsukuba) for valuable discussions.

REFERENCES

(1) Haruta, M.; Kobayashi, T.; Sano, H.; Yamada, N. *Chem. Lett.* **1987**, *16*, 405−408.
(2) Haruta, M. *Catal. Today* **1997**, *36*, 153−166.
(3) Heiz, U.; Landman, U., Eds.; *Nanocatalysis*; Springer: Berlin, Heidelberg, NY, 2007.
(4) Coquet, R.; Howard, K. L.; Willock, D. J. *Chem. Soc. Rev.* **2008**, *37*, 2046−2076.
(5) Haruta, M. *Chem. Rec.* **2003**, *3*, 75−87.
(6) Tsunoyama, H.; Sakurai, H.; Negishi, Y.; Tsukuda, T. *J. Am. Chem. Soc.* **2005**, *127*, 9374−9375.
(7) Turner, M.; Golovko, V. B.; Vaughan, O. P. H; Abdulkin, P.; Berenguer-Murcia, A.; Tikhov, M. S.; Johnson, B. F. G.; Lambert, R. M. *Nature* **2008**, *454*, 981−984.
(8) Herzing, A. A.; Kiely, C. J.; Carley, A. F.; Landon, P.; Hutchings, G. J. *Science* **2008**, *321*, 1331−1335.
(9) Heiz, U.; Sanchez, A.; Abbet, S.; Schneider, W.-D. *J. Am. Chem. Soc.* **1999**, *121*, 3214−3217.
(10) Bonačić-Koutecký, V.; Mitrić, R.; Bürgel, C.; B., S.-B. *Comput. Mater. Sci.* **2006**, *35*, 151−157.
(11) Okumura, M.; Tsubota, S.; Haruta, M. *J. Mol. Catal. A: Chem.* **2003**, *199*, 73−84.
(12) Landman, U.; Yoon, B.; Zhang, C.; Heiz, U.; Arenz, M. *Top. Catal.* **2007**, *44*, 145−158.
(13) Harding, C.; Habibpour, V.; Kunz, S.; Farnbacher, A. N.-S.; Heiz, U.; Yoon, B.; Landman, U. *J. Am. Chem. Soc.* **2009**, *131*, 538−548.
(14) Rodríguez, J. A.; Feria, L.; Jirsak, T.; Takahashi, Y.; Nakamura, K.; Illas, F. *J. Am. Chem. Soc.* **2010**, *132*, 3177−3186.
(15) Haruta, M. *Faraday Discuss.* **2011**, *152*, 11−32.
(16) Howard, K. L.; Willock, D. J. *Faraday Discuss.* **2011**, *152*, 135−151.
(17) Semenikhina, V. V.; Lyalin, A.; Solov'yov, A. V; Greiner, W. *JETP* **2008**, *106*, 678−689.
(18) Dick, V. V.; Solov'yov, I. A.; Solov'yov, A. V. *Phys. Rev. B* **2011**, *84*, 115408.
(19) Yoon, B.; Häkkinen, H.; Landman, U.; Wörz, A. S.; Antonietti, J.-M.; Abbet, S.; Judai, K.; Heiz, U. *Science* **2005**, *307*, 403−407.
(20) Chen, M.; Cai, Y.; Yan, Z.; Goodman, D. W. *J. Am. Chem. Soc.* **2006**, *128*, 6341−6346.
(21) Yoon, B.; Häkkinen, H.; Landman, U. *J. Phys. Chem. A* **2003**, *107*, 4066−4071.
(22) Ding, X.; Li, Z.; Yang, J.; Hou, J. G.; Zhu, Q. *J. Chem. Phys.* **2004**, *120*, 9594−9600.
(23) Fernández, E.; Ordejón, P.; Balbás, L. C. *Chem. Phys. Lett.* **2005**, *408*, 252−257.
(24) Lyalin, A.; Taketsugu, T. *J. Phys. Chem. C* **2009**, *113*, 12930−12934.
(25) Lyalin, A.; Taketsugu, T. *J. Phys. Chem. Lett.* **2010**, *1*, 1752−1757.
(26) Häkkinen, H.; Landman, U. *J. Am. Chem. Soc.* **2001**, *123*, 9704−9705.

(27) Socaciu, L. D.; Hagen, J.; Bernhardt, T. M.; Wöste, L.; Heiz, U.; Häkkinen, H.; Landman, U. *J. Am. Chem. Soc.* **2003**, *125*, 10437−10445.
(28) Häkkinen, H.; Abbet, S.; Sanchez, A.; Heiz, U.; Landman, U. *Angew. Chem., Int. Ed.* **2003**, *42*, 1297−1300.
(29) Varganov, S.; Olson, R. M.; Gordon, M. S.; Metiu, H. *J. Chem. Phys.* **2003**, *119*, 2531−2537.
(30) Roldán, A.; González, S.; Ricart, J. M.; Illas, F. *Chem. Phys. Chem.* **2009**, *10*, 348−351.
(31) Fang, H.-C.; Li, Z. H.; Fan, K.-N. *Phys. Chem. Chem. Phys.* **2011**, *13*, 13358−13369.
(32) Hutchings, G. J. *J. Catal.* **2006**, *242*, 71−81.
(33) Lyalin, A.; Taketsugu, T. *J. Phys. Chem. C* **2010**, *114*, 2484−2493.
(34) Bürgel, C.; Reilly, N. M.; Johnson, G. E.; Mitrićc, R.; Kimble, M. L.; Castleman, A. W., Jr.; Bonačcić-Koutecký, V. *J. Am. Chem. Soc.* **2008**, *130*, 1694−1698.
(35) Sanchez, A.; Abbet, S.; Heiz, U.; Schneider, W.-D.; Hakkinen, H.; Barnett, R. N.; Landman, U. *J. Phys. Chem. A* **1999**, *103*, 9573−9578.
(36) Zhang, C.; Yoon, B.; Landman, U. *J. Am. Chem. Soc.* **2007**, *129*, 2228−2229.
(37) Sterrer, M.; Risse, T.; Pozzoni, U.; Giordano, L.; Heyde, M.; Rust, H.; Pacchioni, G.; Freund, H. *Phys. Rev. Lett.* **2007**, *98*, 096107.
(38) Frondelius, P.; Häkkinen, H.; Honkala, K. *Phys. Rev. B* **2007**, *76*, 073406.
(39) Honkala, K.; Häkkinen, H. *J. Phys. Chem. C* **2007**, *111*, 4319−4327.
(40) Arenal, R.; Stéphan, O.; Kociak, M.; Taverna, D.; Loiseau, A.; Colliex, C. *Phys. Rev. Lett.* **2005**, *95*, 127601/1−4.
(41) Golberg, D.; Bando, Y.; Huang, Y.; Terao, T.; Mitome, M.; Tang, C.; Zhi, C. *ACS Nano* **2010**, *4*, 2979−2993.
(42) Note that a change in structural properties of gold clusters has been found for clusters supported on h-BN nanomesh—a h-BN monolayer deposited on transition metal surfaces, like Rh(111) or Pt(111).[78] In this case, however, the deposited h-BN monolayer is corrugated, and its structural and electronic properties can be considerably modified by the metal.[50,79]
(43) Gao, M.; Lyalin, A.; Taketsugu, T. *Catalysts* **2011**, *1*, 18−39.
(44) Wu, Z.; Cohen, R. E. *Phys. Rev. B* **2006**, *73*, 235116/1−6.
(45) Sánchez-Portal, D.; Ordejón, P.; Artacho, E.; Soler, J. M. *Int. J. Quantum Chem.* **1997**, *65*, 453−461.
(46) Soler, J. M.; Artacho, E.; Gale, J. D.; García, A.; Junquera, J.; Ordejón, P.; Sánchez-Portal, D. *J. Phys.: Condens. Matter* **2002**, *14*, 2745−2779.
(47) Sánchez-Portal, D.; Ordejón, P.; Canadell, E. *Struct. Bonding (Berlin, Ger.)* **2004**, *113*, 103−170.
(48) Tran, F.; Laskowski, R.; Blaha, P.; Schwarz, K. *Phys. Rev. B* **2007**, *75*, 115131.
(49) Perdew, J. P.; Burke, K.; Ernzerhof, M. *Phys. Rev. Lett.* **1996**, *77*, 3865−3868.
(50) Laskowski, R.; Blaha, P.; Schwarz, K. *Phys. Rev. B* **2008**, *78*, 045409/1−10.
(51) Laskowski, R.; Blaha, P. *Phys. Rev. B* **2010**, *81*, 075418.
(52) Artacho, E.; Sánchez-Portal, D.; Ordejón, P.; García, A.; Soler, J. M. *Phys. Status Solidi B* **1999**, *215*, 809−817.
(53) Junquera, J.; Paz, O.; Sánchez-Portal, D.; Artacho, E. *Phys. Rev. B* **2001**, *64*, 235111/1−9.
(54) Troullier, N.; Martins, J. L. *Phys. Rev. B* **1991**, *43*, 1993−2006.
(55) Kleinman, L.; Bylander, D. M. *Phys. Rev. Lett.* **1982**, *48*, 1425−1428.
(56) Fernández, E.; Soler, J. M.; Garzón, I. L.; Balbás, L. C. *Phys. Rev. B* **2004**, *70*, 165403/1−14.
(57) Torres, M. B.; Fernández, E. M.; Balbás, L. C. *Phys. Rev. B* **2005**, *71*, 155412.
(58) Coquet, R.; Hutchings, G. J.; Taylor, S. H.; Willock, D. J. *J. Mater. Chem.* **2006**, *16*, 1978−1988.
(59) Bader, R. *Atoms in Molecules: A Quantum Theory*; Oxford University Press: New York, 1990.
(60) Henkelman, G.; Arnaldsson, A.; Jònsson, H. *Comput. Mater. Sci.* **2006**, *36*, 354−360.
(61) Kokalj, A. *Comput. Mater. Sci.* **2003**, *28*, 155−168.
(62) Huber, K. P.; Herzberg, G. *Molecular Spectra and Molecular Structure Constants of Diatomic Molecules*; Van Nostrand Reinhold: New York, 1979.
(63) Monkhorst, H. J.; Pack, J. D. *Phys. Rev. B* **1976**, *13*, 5188.
(64) Yoo, C. S.; Akella, J.; Cynn, H.; Nicol, M. *Phys. Rev. B* **1997**, *56*, 140−146.
(65) Furthmüller, J.; Hafner, J.; Kresse, G. *Phys. Rev. B* **1994**, *50*, 15606−15622.
(66) Azevedo, S.; Kaschny, J. R.; de Castilho, C. M.; de Brito Mota, F. *Eur. Phys. J. B* **2009**, *67*, 507−512.
(67) Orellana, W.; Chacham, H. *Phys. Rev. B* **2001**, *63*, 125205.
(68) Kuzubov, A. A.; Serzhantova, M. V.; Fedorov, A. S.; Tomilin, F. N.; Kozhevnikova, T. A. *JETP Lett.* **2011**, *93*, 335−338.
(69) Si, M. S.; Li, J. Y.; Shi, H. G.; Niu, X. N.; Xue, D. S. *Europhys. Lett.* **2009**, *86*, 46002/1−6.
(70) Zobelli, A.; Ewels, C. P.; Gloter, A.; Seifert, G.; Stephan, O.; Csillag, S.; Colliex, C. *Nano Lett.* **2006**, *6*, 1955−1960.
(71) Jin, C.; Lin, F.; Suenaga, K.; Iijima, S. *Phys. Rev. Lett.* **2009**, *102*, 195505.
(72) Yin, L.-C.; Cheng, H.-M.; Saito, R. *Phys. Rev. B* **2010**, *81*, 153407.
(73) Lyalin, A.; Taketsugu, T. *Faraday Discuss.* **2011**, *152*, 185−201.
(74) Caballero, R.; Quintanar, C.; Köster, A. M.; Khanna, S. N.; Reveles, J. U. *J. Phys. Chem. C* **2008**, *112*, 14919−14928.
(75) The effect of the strong influence on the binding and activation of O_2 by Au, which comes from a weak interaction with the defect-free h-BN surface, is unusual. Therefore, we have performed an additional test of our results using the more popular PBE functional. We have considered only one layer of h-BN as a model for the h-BN surface because the PBE functional can not reproduce binding between layers in h-BN. Our calculations demonstrate that binding energies of O_2 to a free Au and Au_2 obtained within the PBE approximation are 0.36 eV (0.49 eV) and 0.33 eV (0.48 eV), respectively. Numbers in parentheses correspond to the WC results. All data were corrected on BSSE. The calculated binding energies of O_2 to a supported Au and Au_2 are 0.81 eV (1.05 eV) and 0.19 eV (0.28 eV), respectively. The binding energies of Au and Au_2 to the defect-free h-BN surface are 0.07 eV (0.25 eV) and 0.50 eV (0.77 eV), respectively. Thus, binding energies calculated with the use of the PBE functional are systematically lower than those obtained with the use of the WC functional by approximately 0.2 eV. However, geometries and all qualitative features of O_2 adsorption on free and supported Au and Au_2 remain unchanged. Thus, results obtained within the PBE approximation demonstrate strong enhancement of O_2 adsorption and activation on the Au atom supported on the defect-free h-BN surface.
(76) Lang, S. M.; Bernhardt, T. M.; Barnett, R. N.; Yoon, B.; Landman, U. *J. Am. Chem. Soc.* **2009**, *131*, 8939−8951.
(77) Fujitani, T.; Nakamura, I.; Akita, T.; Okumura, M.; Haruta, M. *Angew. Chem., Int. Ed.* **2009**, *48*, 9515−9518.
(78) Ng, M. L.; Preobrajenski, A. B.; Vinogradov, A. S.; Møartensson, N. *Surf. Sci.* **2008**, *602*, 1250−1255.
(79) Preobrajenski, A. B.; Vinogradov, A. S.; Møartensson, N. *Surf. Sci.* **2005**, *582*, 21−30.